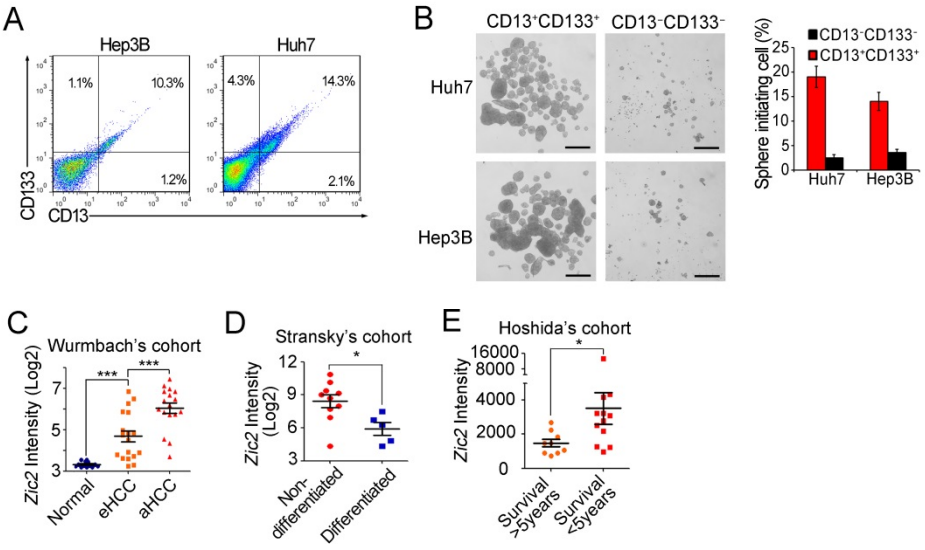

Supplemental Figure 1. Zic2 expression profiles in liver cancer cells. (A) $CD13^{+}CD133^{+}$ liver CSCs were sorted from Hep3B and Huh7 cells using a FACS assay. (B) $CD13^{+}CD133^{+}$ and $CD13^{-}CD133^{-}$ cells were analyzed for self-renewal by sphere formation assays. Scale bar, 500 μm. (C) Using R language and Bioconductor methods, we analyzed *Zic2* expression in HCC tumor and peri-tumor tissues provided by Wurmbach's cohort. eHCC: early HCC; aHCC: advanced HCC. (D) *Zic2* is highly expressed in non-differentiated HCC cell lines (HLE, HLF, JHH-6, SK-HEP-1, SNU-182, SNU-387, SNU-398, SNU-423, SNU-449 and SNU-475) compared to differentiated cell lines (C3A, Hep 3B2.1-7, Hep G2, HuH-6 and HuH-7) from Stransky's cohort. (E) High expression of Zic2 was consistent with poor prognosis provided Hoshida's cohort. Data are shown as means ± SD. Two tailed Student's t-test was used for statistical analysis, *, $P < 0.05$; ***, $P < 0.001$. P value less than 0.05 was considered significant. Data are representative of at least three independent experiments.

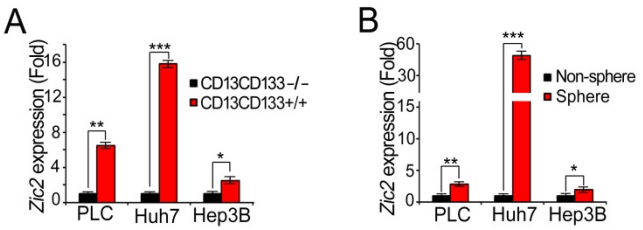

Supplemental Figure 2. Zic2 is highly expressed in liver CSCs. (A, B) Increased expression of *Zic2* in $CD13^{+}CD133^{+}$ liver CSCs (A) and oncospheres (B) derived from HCC cell lines (PLC, Huh7 and Hep3B). Data are shown as means ± SD. Two tailed Student's t-test was used for statistical analysis, *, $P < 0.05$; **, $P < 0.01$; ***, $P < 0.001$. P value less than 0.05 was considered significant. Data are representative of at least three independent experiments.

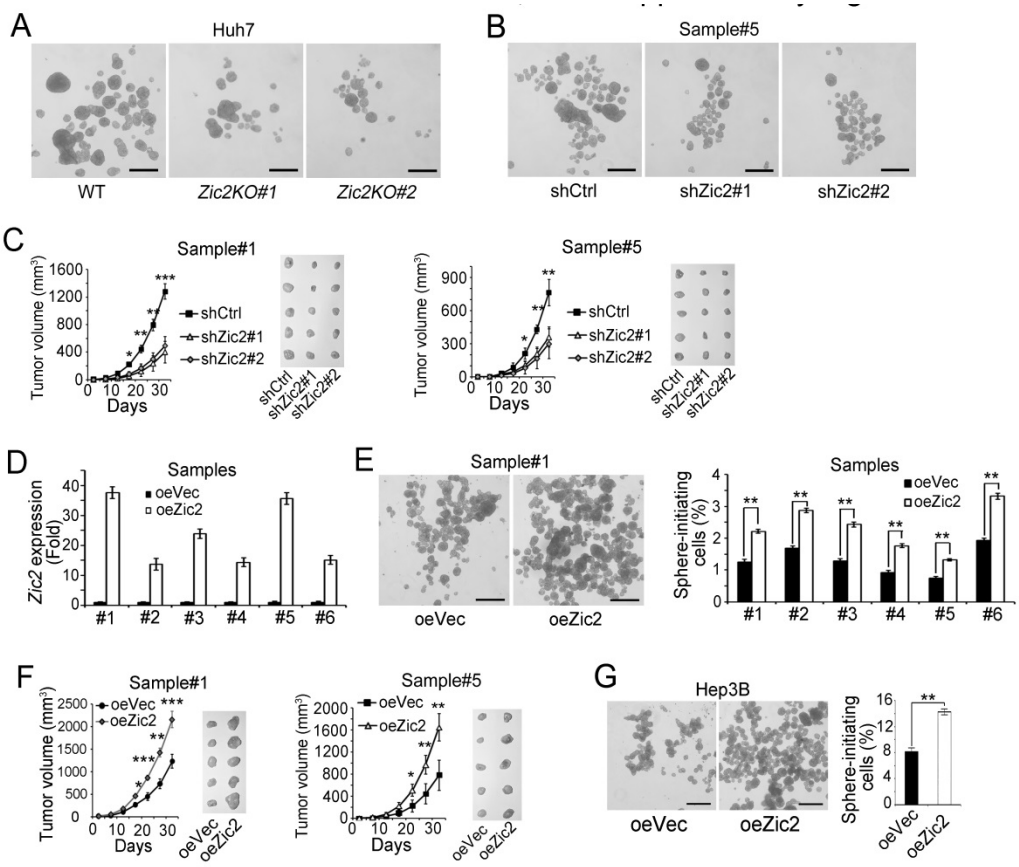

Supplemental Figure 3. Zic2 enhances sphere formation capacity of liver CSCs. (A) *Zic2* deficient Huh7 cells were established using CRISPR/Cas9 approach and cultured for sphere formation assay. (B) Zic2 was silenced in HCC samples and cultured for sphere formation assay. (C) Zic2 silenced and shCtrl treated cells (1×10^6) from HCC samples were injected into BALB/c nude mice, and tumor volume was measured every five days. Six HCC samples achieved similar results. (D) Zic2 overexpressing primary cells were established. oeVec: overexpression vector; oeZic2: overexpression Zic2. (E) Zic2 overexpressing and control primary cells were cultured for sphere formation. (F) Zic2 overexpressing primary cells (1×10^6) were injected into BALB/c nude mice for xenograft assays. (G) Increased sphere formation capacity was observed in Zic2 overexpressing Hep3B cells. Scale bars, A, B, E, G, 500 μm. Data are shown as means ± SD. Two tailed Student's t-test was used for statistical analysis, *, $P < 0.05$; **, $P < 0.01$; ***, $P < 0.001$. P value less than 0.05 was considered significant. Data are representative of at least three independent experiments.

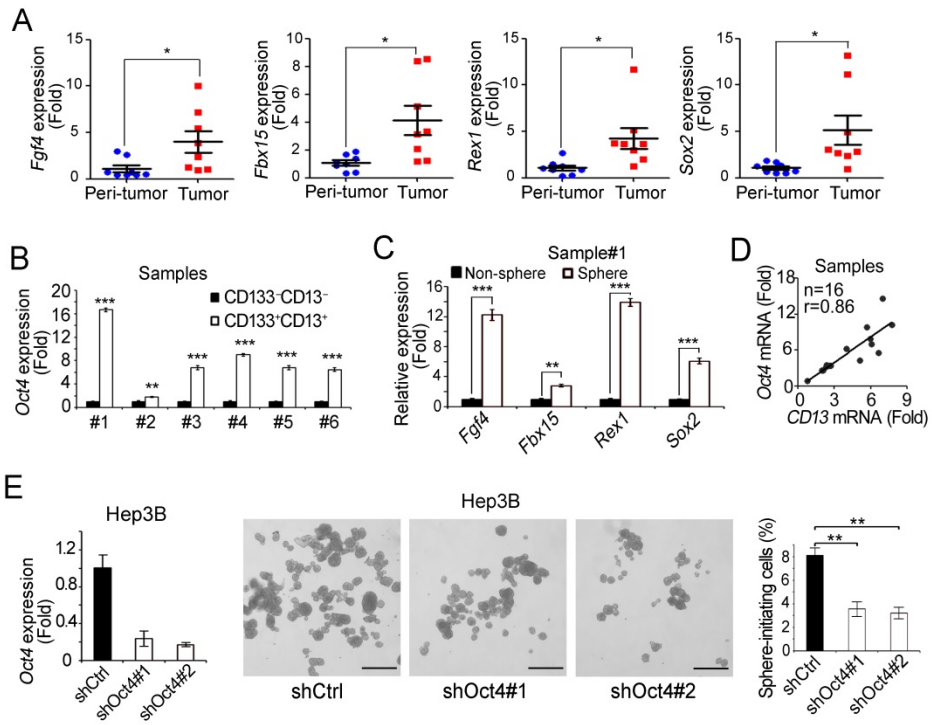

Supplemental Figure 4. Oct4 signaling is required for liver CSCs. (A) High expression levels of *Oct4* target genes in human HCC samples. (B) *Oct4* is highly expressed in sorted $CD13^{+}CD133^{+}$ HCC primary cells. (C) Oct4 signaling is activated in oncospheres. (D) Correlation analysis of *Oct4* and *CD13* were performed from their expression levels by realtime PCR. (E) Oct4 was silenced in Hep3B cells followed by sphere formation assays. Scale bar, 500 μm. Data are shown as means ± SD. Two tailed Student's t-test was used for statistical analysis, *, $P < 0.05$; **, $P < 0.01$; ***, $P < 0.001$. P value less than 0.05 was considered significant. Data are representative of at least three independent experiments.

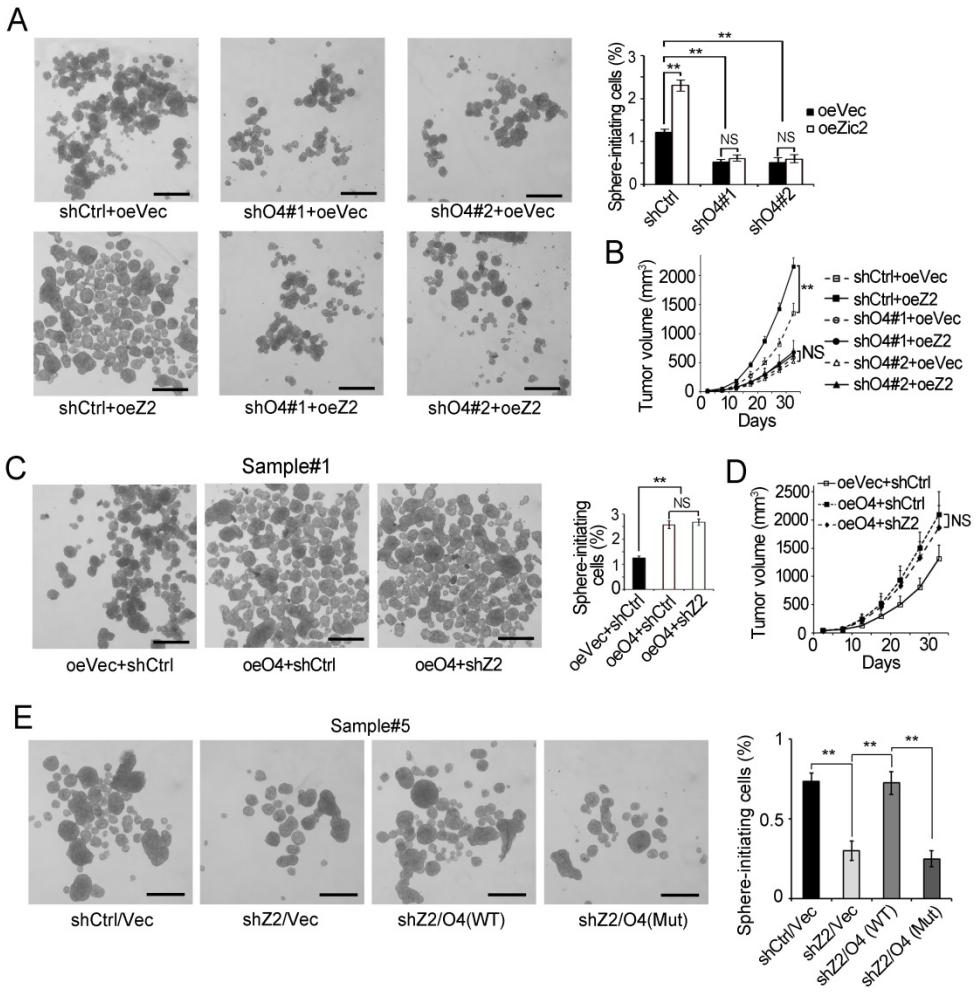

Supplemental Figure 5. Zic2 drives self-renewal of liver CSCs through Oct4 signaling. (A, B) Sphere formation capacity (A) and xenograft tumor propagation (B) were detected in the indicated Oct4 silenced HCC primary cells. (C, D) Sphere formation (C) and xenograft tumor propagation (D) were detected in the indicated cells. (E) Zic2 depleted HCC primary cells were established and rescued with WT Oct4 and dominant negative mutant Oct4, then self-renewal was measured in sphere formation medium. WT, wild type; Mut, mutant. Scale bar, A, C, E, 500 μm. Data are shown as means ± SD. Two tailed Student's t-test was used for statistical analysis, *, $P < 0.05$; **, $P < 0.01$; ***, $P < 0.001$. P value less than 0.05 was considered significant. Data are representative of at least three independent experiments.

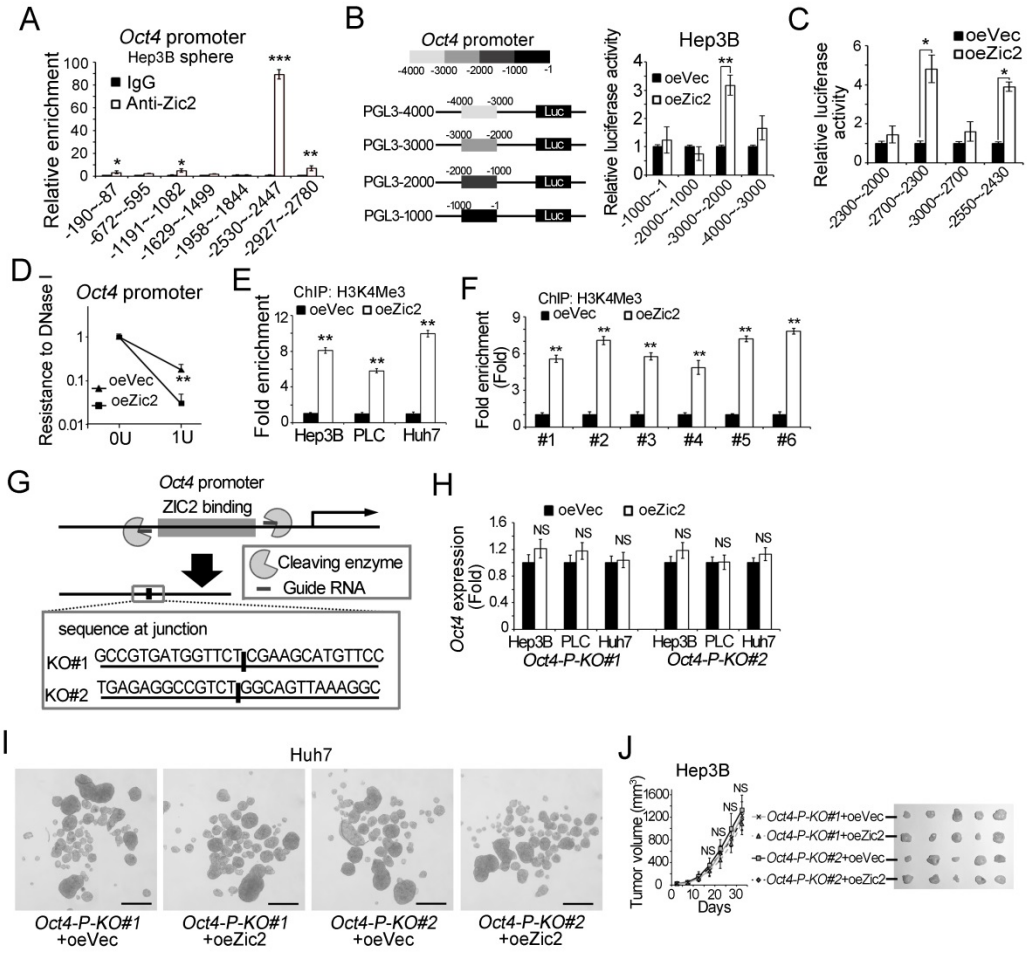

Supplemental Figure 6. Zic2 binds to *Oct4* promoter. (A) Oncospheres derived from Hep3B cells were used for ChIP assay, followed by analyzing the enrichment of *Oct4* promoter by realtime PCR. (B, C) Zic2 enhances the activation of *Oct4* promoter. The indicated regions of *Oct4* promoter were constructed for luciferase reporter assays. (D-F) Zic2 overexpression increases chromatin accessibility at the *Oct4* locus (D) and elevates H3K4Me3 levels (E, F). (G) The Zic2 binding sequence of *Oct4* promoter was deleted in HCC cell lines using a CRISPER/Cas9 lentivirus system. Selected cell clones were confirmed by DNA sequencing as presented within small black box (lower panel). Bold lines denote junction sites. (H) Oct4 expression was examined in the indicated cells. (I) Oct4 promoter CR4 deleted Huh7 cells were established and then overexpressed Zic2, and self-renewal capacity was evaluated using sphere formation medium. *Oct4-P-KO*, *Oct4* promoter CR4 knockout, oeZic2, overexpressing Zic2. Scale bar, 500 μm. (J) Enograft tumor propagation was analyzed in the Zic2 binding sequence of *Oct4* promoter deficient cells. Data are shown as means ± SD. Two tailed Student's t-test was used for statistical analysis, *, $P < 0.05$; **, $P < 0.01$; ***, $P < 0.001$. P value less than 0.05 was considered significant. Data are representative of at least three independent experiments.

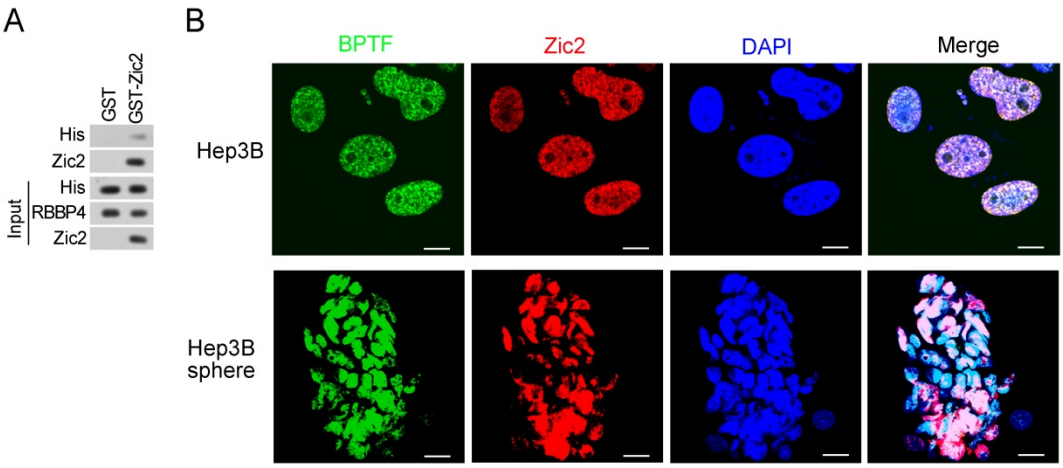

Supplemental Figure 7. BPTF interacts with Zic2. (A) Recombinant GST-Zic2 and His-RBBP4 proteins were incubated for pulldown assays. (B) Hep3B cells and spheres were stained with BPTF and Zic2, counterstained with DAPI. Scale bars: 3 μm for Hep3B, 10 μm for spheres. Data are representative of at least three independent experiments.

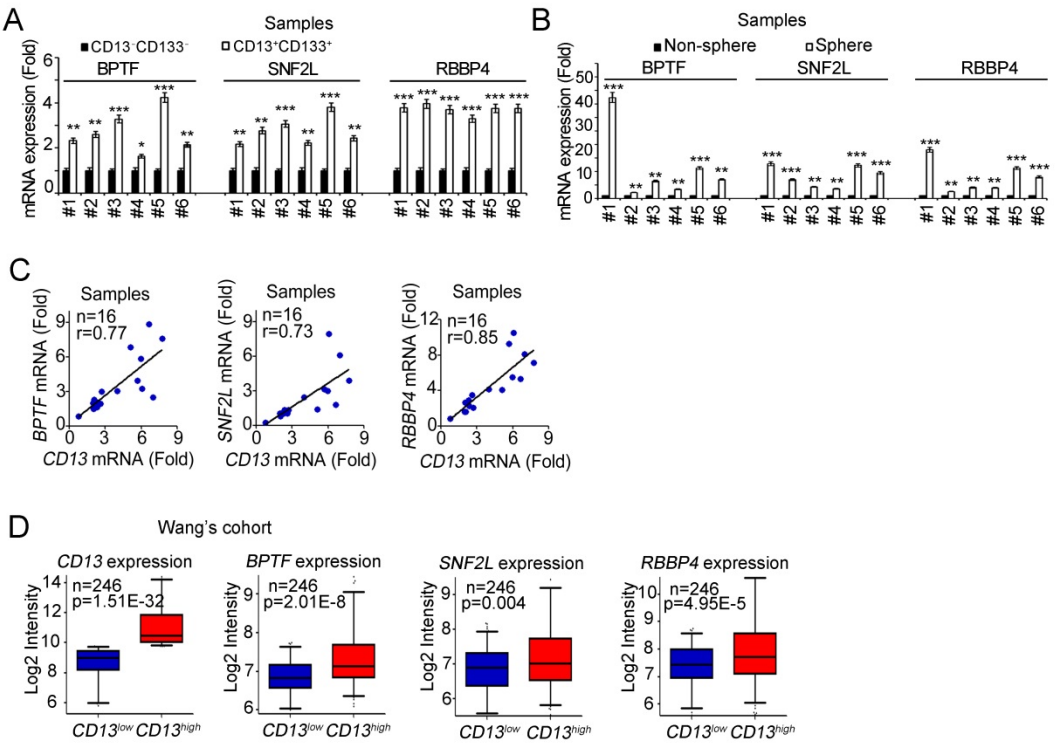

Supplemental Figure 8. The NURF complex is highly expressed in liver CSCs. (A, B) The NURF components were detected in liver CSCs and oncospheres by realtime PCR. Data are shown as means ± SD. (C) The NURF complex expression levels are positively related to *CD13* expression in HCC samples. mRNA levels of *CD13* and the NURF complex were detected by qPCR and shown as fold changes relative to peri-tumor tissues. (D) The NURF complex is highly expressed in $CD13^{high}$ HCC samples. HCC samples (GSE14520) were divided into two subpopulations according to *CD13* expression levels, followed by analyzing the expression of NURF complex. For A, B, data are shown as means ± SD. Two tailed Student's t-test was used for statistical analysis, *, $P < 0.05$; **, $P < 0.01$; ***, $P < 0.001$. *P* value less than 0.05 was considered significant. For D, data are shown as box and whisker plot (5-95 percentile). Whiskers below and above boxes extend to the 5th and 95th percentiles, respectively. Horizontal lines within boxes represent median levels of gene intensity. Boxes represent interquartile range (IQR); upper and lower edge corresponds to the 75th and 25th percentiles, respectively. Data are representative of at least three independent experiments.

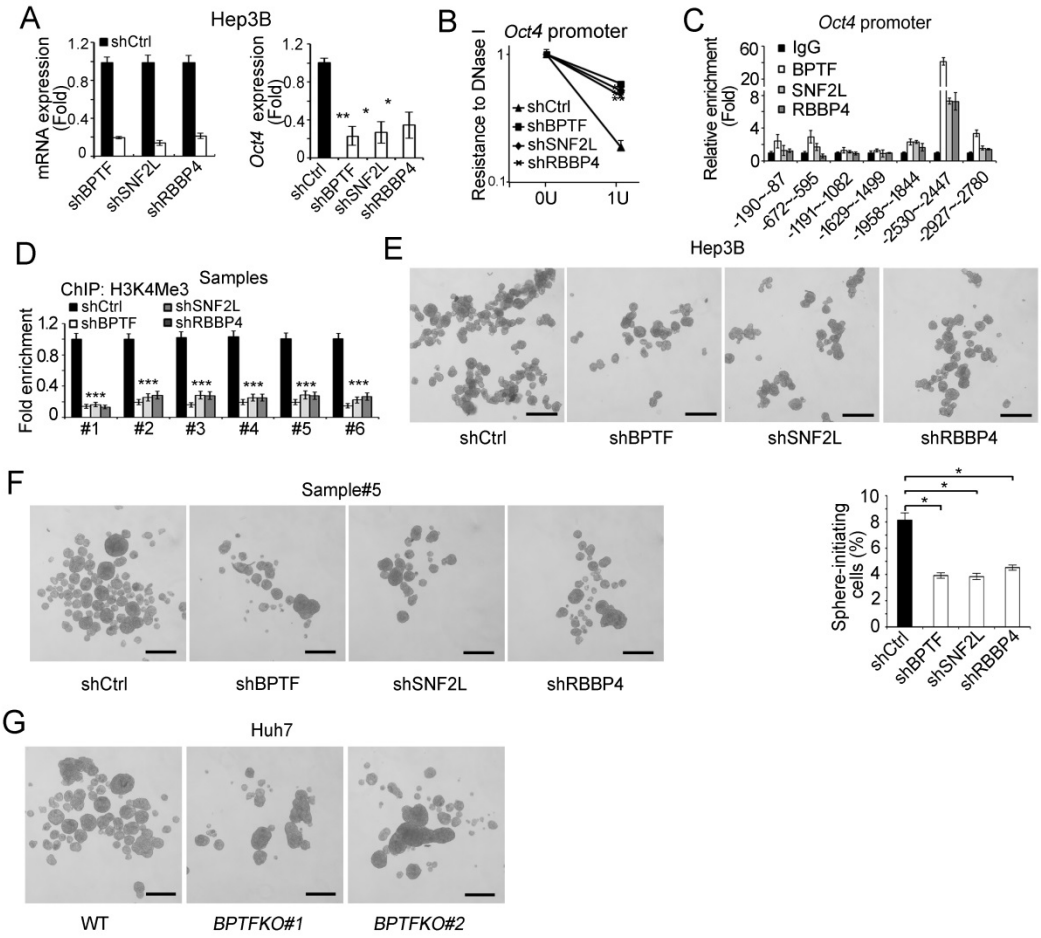

Supplemental Figure 9. The NURF complex is required for self-renewal of liver CSCs. (A) NURF complex knockdown reduces *Oct4* expression in Hep3B cells. (B) The NURF complex augments chromatin accessibility of the *Oct4* locus. NURF complex silenced cell nuclei were extracted followed by DNase I digestion. (C) The NURF complex binds to the CR4 region of the *Oct4* promoter through ChIP assays. (D) Knockdown of NURF complex decreases H3K4 tri-methylation levels at the *Oct4* locus in HCC primary cells. (E) NURF silenced Hep3B cells were cultured for sphere formation. (F) NURF complex depletion reduced sphere formation of HCC primary cells. (G) BPTF deficient Huh7 cells impaired their self-renewal capacity. Scale bar, E, F, G, 500 μm. Data are shown as means ± SD. Two tailed Student's t-test was used for statistical analysis, *, $P < 0.05$; **, $P < 0.01$; ***, $P < 0.001$. P value less than 0.05 was considered significant. Data are representative of at least three independent experiments.

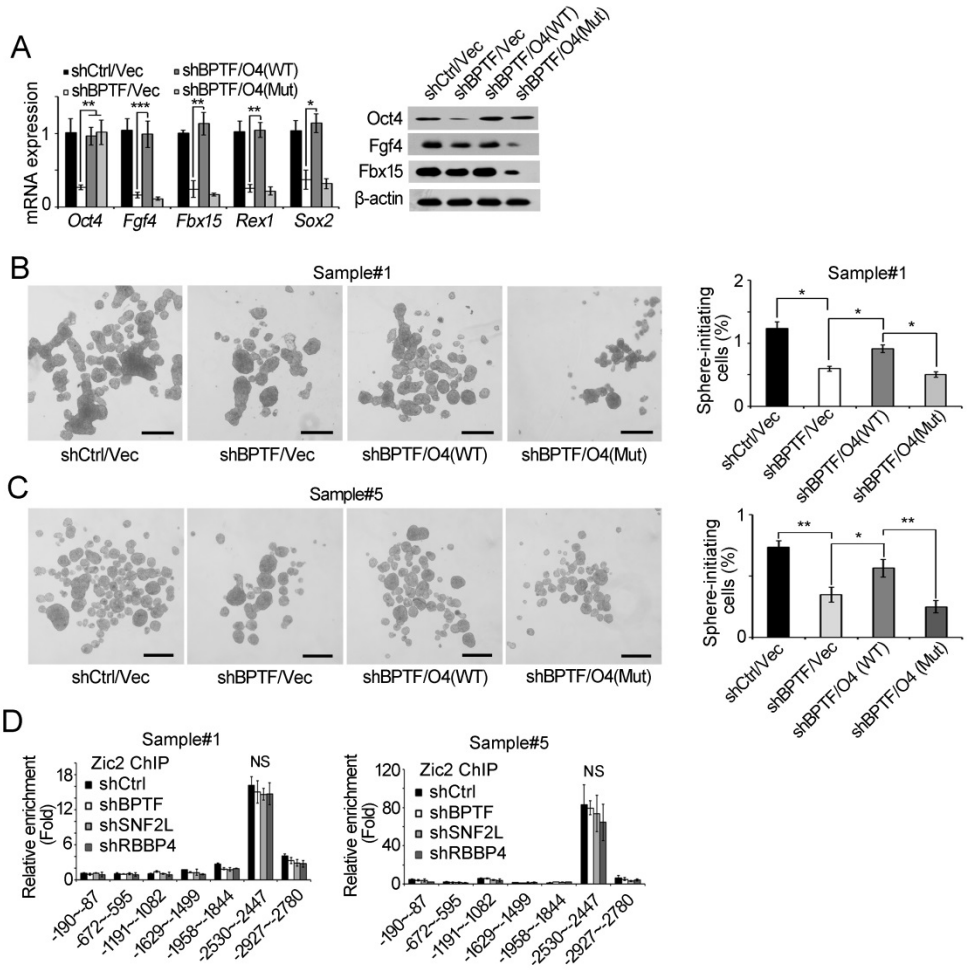

Supplemental Figure 10. BPTF drives self-renewal of liver CSCs through Oct4 signaling. (A-C) NURF depleted primary cells were rescued with functional Oct4 or mutant Oct4. *S*phere formation capacity and expression levels of the indicated genes were analyzed. O4, Oct4. (D NURF depleted and shCtrl treated HCC primary cells were incubated with anti-Zic2 antibody for ChIP assay, then the indicated regions of *Oct4* promoter were analyzed by realtime PCR. Scale bar, C, D, 500 μm. Data are shown as means ± SD. Two tailed Student's t-test was used for statistical analysis, NS, not significant; *, $P < 0.05$; **, $P < 0.01$. P value less than 0.05 was considered significant. Data are representative of at least three independent experiments.

Figure 1D

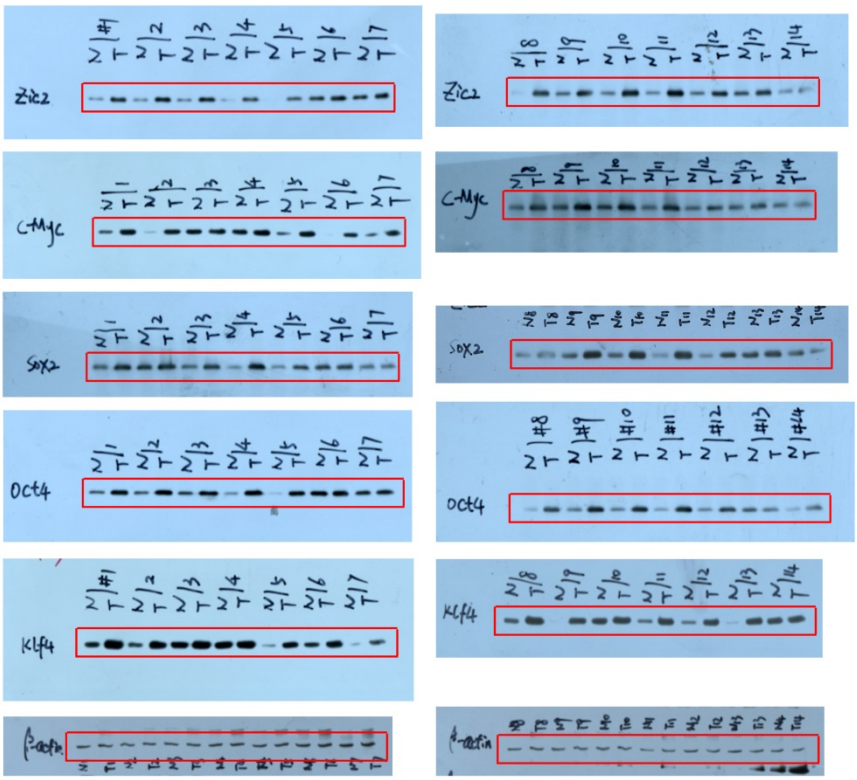

Supplemental Figure 11: Uncropped blots for Figure 1. Red boxes indicate blot images shown in the according figures.

Figure 2C

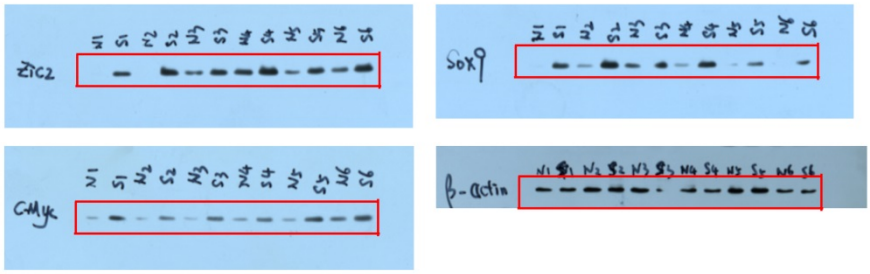

Uncropped blots for Figure 2. Red boxes indicate blot images shown in the according figures.

Figure3A

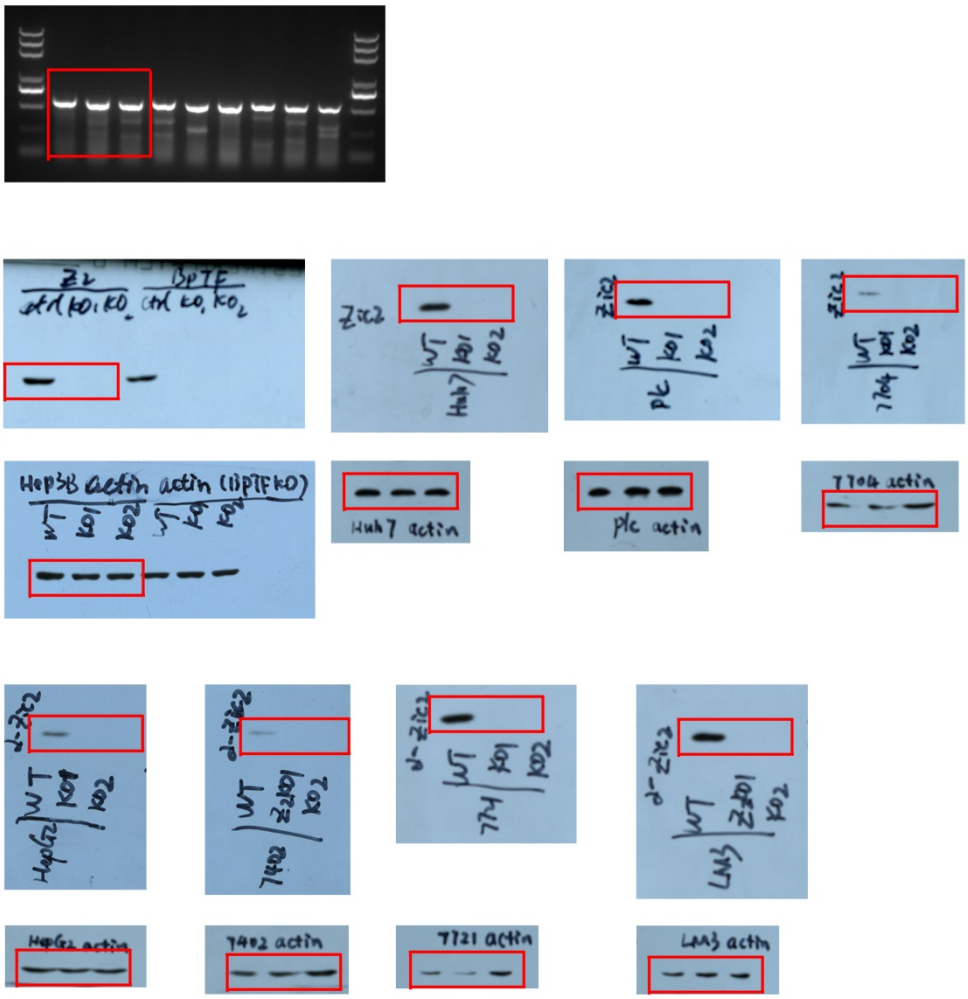

Uncropped gel and blots for Figure 3. Red boxes indicate blot and gel images shown in the according figures.

Figure 4B

Uncropped blots for Figure 4. Red boxes indicate blot images shown in the according figures.

Figure 5E

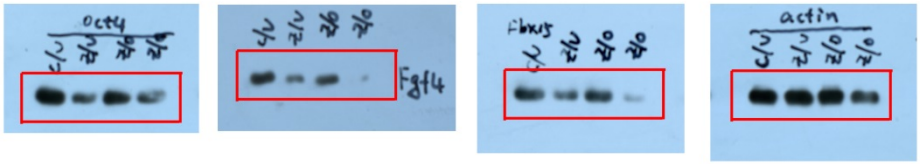

Uncropped blots for Figure 5. Red boxes indicate blot images shown in the according figures.

Figure 6B

Uncropped blot for Figure 6. Red box indicates blot image shown in the according figure.

Figure 7B

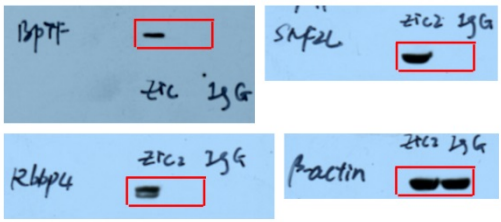

Figure 7C

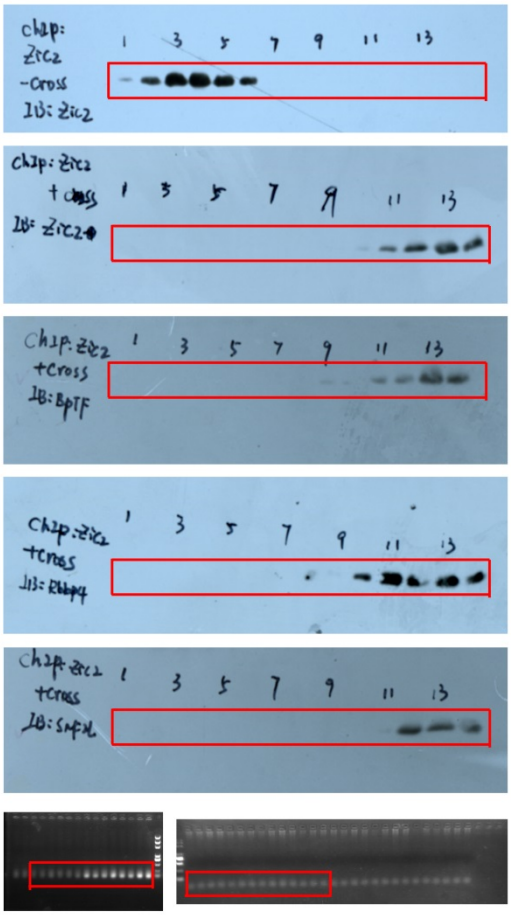

Figure 7D

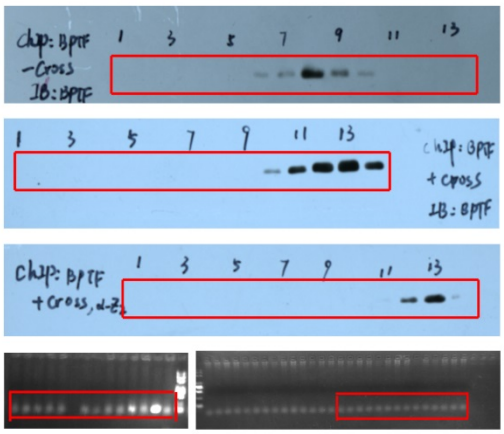

Uncropped blots and gels for Figure 7. Red boxes indicate blot and gel images shown in the according figures.

Figure 8D

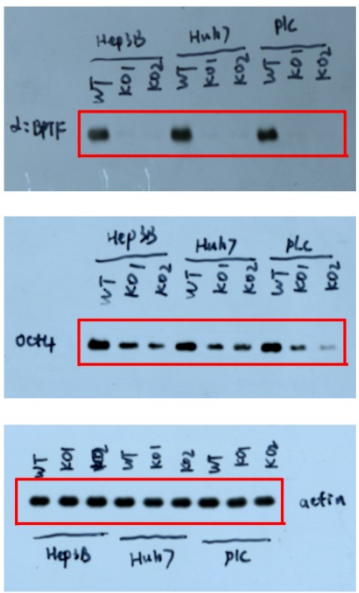

Uncropped blots for Figure 8. Red boxes indicate blot images shown in the according figures.

Figure 9C

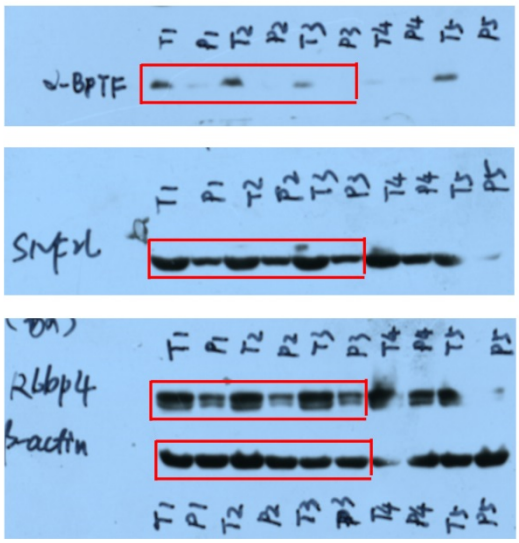

Uncropped blots for Figure 9. Red boxes indicate blot images shown in the according figures.

Supplementary Figure 7A

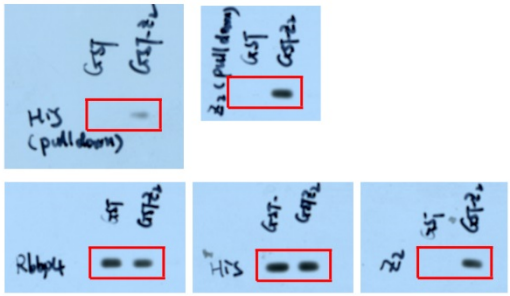

Uncropped blots for Supplemental Figure 7. Red boxes indicate blot images shown in the according figures.

Supplementary Figure 10A

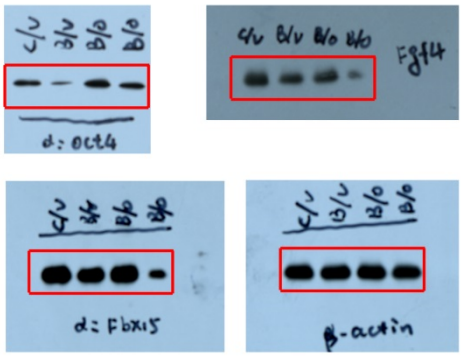

Uncropped blots for Supplemental Figure 10. Red boxes indicate blot images shown in the according figures.

Supplemental Table 1

Table 1A. Frequencies of tumor initiating cells of Zic2 knockout

Cell	CSC ratio (95% CI)	*P* value
WT (A)	1/791 (1/1979-1/316)	
Zic2KO#1 (B)	1/5718 (1/13812-1/2367)	0.001 (B *vs* A)
Zic2KO#2 (C)	1/4601 (1/11105-1/1907)	0.005 (C *vs* A)

Table 1B. Frequencies of tumor initiating cells of Oct4 depletion

Cell	CSC ratio (95% CI)	*P* value
shCtrl (A)	1/571 (1/1380-1/236)	
shOct4#1 (B)	1/3849 (1/9424-1/1572)	0.001 (B *vs* A)
shOct4#2 (C)	1/4825 (1/11627-1/2002)	0.0003 (C *vs* A)

Table 1C. Frequencies of tumor initiating cells of the NURF complex depletion

Cell	CSC ratio (95% CI)	*P* value
shCtrl (A)	1/571 (1/1380-1/236)	
shBPTF (B)	1/5718 (1/13812-1/2367)	0.0001 (B *vs* A)
shSNF2L (C)	1/4601 (1/11105-1/1907)	0.0007 (C *vs* A)
shRBBP4 (D)	1/4825 (1/11627-1/2002)	0.0003 (D *vs* A)

The indicated cells were established and then performed sphere formation. Two weeks later, the spheres were digested into single-cell suspension and then subcutaneously implanted 1×10^4, 1×10^3, 1×10^2 and 10 cells into BALB/c nude mice. Frequencies of tumor initiating cells were calculated using extreme limiting dilution analysis. 95% CI, 95% confidence interval of the estimation; vs, versus. *P* value less than 0.05 was considered significant.

Supplemental Table 2. Realtime PCR primers used in this study

Primers	Sequences
18S (Forward)	5'-AACCCGTTGAACCCCATT-3'
18S (Reverse)	5'-CCATCCAATCGGTAGTAGCG-3'
actin (Forward)	5'-TCCATCATGAAGTGTGACGT-3'
actin (Reverse)	5'-GAGCAATGATCTTGATCTTCAT-3'
Zic2 (Forward)	5'-AACTCCACAACCAGTACGGC-3'
Zic2 (Reverse)	5'-AGCCCTCAAACTCACACTGG-3'
Oct4 (Forward)	5'-CTGGGTTGATCCTCGGACCT-3'
Oct4 (Reverse)	5'-CCATCGGAGTTGCTCTCCA-3'
CD13 (Forward)	5'-GACCAAAGTAAAGCGTGGAATCG-3'
CD13 (Reverse)	5'-TCTCAGCGTCACCCGGTAG-3'
Sox2 (Forward)	5'-GCCGAGTGGAAACTTTTGTCG-3'
Sox2 (Reverse)	5'-GGCAGCGTGTACTTATCCTTCT-3'
Nanog (Forward)	5'-TTTGTGGGCCTGAAGAAAACT-3'
Nanog (Reverse)	5'-AGGGCTGTCCTGAATAAGCAG-3'
c-Myc (Forward)	5'-GGCTCCTGGCAAAAGGTCA-3'
c-Myc (Reverse)	5'-CTGCGTAGTTGTGCTGATGT-3'
Klf4 (Forward)	5'-CCCACATGAAGCGACTTCCC-3'
Klf4 (Reverse)	5'-CAGGTCCAGGAGATCGTTGAA-3'
Fgf4 (Forward)	5'-AGCAAGGGCAAGCTCTATGG-3'
Fgf4 (Reverse)	5'-CTCGGTTCCCCTTCTTGGTC-3'
Fbx15 (Forward)	5'-GCCATGCCTAGCATCATTGTC-3'
Fbx15 (Reverse)	5'-TGGGAGTTTTATACCAGTCGGT-3'
Rex1 (Forward)	5'-TCACAGTCCAGCAGGTGTTTG-3'
Rex1 (Reverse)	5'-TCTTGTCTTTGCCCGTTTCT-3'
BPTF (Forward)	5'-CTTCAGGAGCCATAGTACCTACA-3'
BPTF (Reverse)	5'-CAAGGGGCGGGATGTCTTTTT-3'
SNF2L (Forward)	5'-GATGCGACCGCCACTATCG-3'
SNF2L (Reverse)	5'-ATTTAGGCGCTTTAGCAGCAA-3'
RBBP4 (Forward)	5'-ATGACCCATGCTCTGGAGTG-3'
RBBP4 (Reverse)	5'-GGACAAGTCGATGAATGCTGAAA-3'
-109 (Forward) (Oct4p)	5'-TTGCCACCACCATTAGGCAA-3'
-87 (Reverse) (Oct4p)	5'-CACCCACTAGCCTTGACCTC-3'
-672(Forward) (Oct4p)	5'-AAGCACCTGGGTTCCTGAAG-3'
-595 (Reverse) (Oct4p)	5'-CACTCTCTCAGGCTCTGCAC-3'
-1191(Forward) (Oct4p)	5'-GGGAGCAAGGAACCTGATGTG-3'
-1082(Reverse) (Oct4p)	5'-TTTGGACTGACTGGG CCTC-3'
-1629(Forward) (Oct4p)	5'-AGATACCTAGGTCCCTGTGG-3'
-1499 (Reverse) (Oct4p)	5'-AGTCCCAATCCCCTCACACAG-3'
-1958(Forward) (Oct4p)	5'-GGCCCTCCACTGAGATCAAG -3'
-1844 (Reverse) (Oct4p)	5'-CATGCTGCTGGTCTAGTGCTT-3'
-2530(Forward) (Oct4p)	5'-AGAGGCCGTCTTCTTGGCAG-3'
-2447 (Reverse) (Oct4p)	5'-CCCAGCCATCTCAATCCCCAG-3'
-2927(Forward) (Oct4p)	5'-TGCCTCAACCTCCCATCAG -3'
-2780 (Reverse) (Oct4p)	5'-AGAGGGACGCAGACAAGG-3'

Oct4p: Oct4 promoter.

Supplemental Table 3. shRNA sequences used in this study

shRNA	Sequences
Zic2-1#	5’-GCAGGAGCTAATCTGCAAG-3’
Zic2-2#	5’-GCCCTATCTCTGCAAGATG-3'
Oct4-1#	5’-GCTTCAAGAACATGTGTAA-3’
Oct4-2#	5’-GGAGGAAGCTGACAACAAT-3’
BPTF	5’-GCATAATGCTGTAATAGAA-3’
SNF2L	5’-GGACTGAATTGGTTGATCT-3’
RBBP4	5’-GAACTGCCTTTCTTTCAAT-3’